Boletim da Sociedade Astronômica Brasileira, **37**, no. 1, 30-31
© SAB 2026

Analysis of the Infrared Spectrum of Planetary Nebulae Observed with the Spitzer Space Telescope

A. L. Silva[1], H. Monteiro[1], & I. Aleman[3]

[1] Universidade Federal de Itajubá e-mail: andreluizpts.al@gmail.com, hmonteiro@unifei.edu.br
[2] Laboratório Nacional de Astrofísica e-mail: ialeman@lna.br

Abstract. Planetary Nebulae (PNs) represent a phase in the evolution of stars with masses between 1 and 8 solar masses, originating from mass loss during the nuclear fusion phase. This study focuses on the analysis of the mid-infrared (MIR) spectrum of six PNs observed by the Spitzer Space Telescope in order to study the line emissions of their spectra and use photoionization models to study the ratios between emission lines and obtain physical information about the objects. Reduced spectra from CASSIS database were used. The identification of emission lines and the measurement of fluxes were performed with the PAHFIT routine, which decomposes the MIR spectrum into components: atomic, molecular, solid, and dust emissions. Photoionization models were calculated with the CLOUDY code. An analysis of the ionization potential of the the central stars of each NP was performed using the $[NeIII]_{15.5\mu m}/[NeII]_{12.8\mu m}$ and $[ArIII]_{8.9\mu m}/[ArII]_{6.9\mu m}$ ratios. Temperature ranges of the central star of each NP were also obtained. Finally it was concluded that there is a certain proportionality between the ionic ratios and the temperature of the stars, but this prediction may be crude for some temperature ranges due to the behavior of the curve formed by the relationship between the temperature and the ratios.

Resumo. Nebulosas planetárias (NPs) representam uma fase na evolução de estrelas com massas entre 1 e 8 massas solares, originadas da perda de massa durante a fase de fusão nuclear. Este estudo concentra-se na análise do espectro no infravermelho médio (IR médio) de seis NPs observadas pelo Telescópio Espacial Spitzer, com o objetivo de estudar as linhas de emissão em seus espectros e utilizar modelos de fotoionização para analisar as razões entre as linhas de emissão e obter informações físicas sobre os objetos. Foram utilizados espectros reduzidos do banco de dados CASSIS. A identificação das linhas de emissão e a medição dos fluxos foram realizadas com a rotina PAHFIT, que decompõe o espectro IR médio em componentes: emissões atômicas, moleculares, sólidas e de poeira. Os modelos de fotoionização foram calculados com o código CLOUDY. Foi realizada uma análise do potencial de ionização das estrelas centrais de cada nanopartícula usando as razões $[NeIII]_{15,5\mu m}/[NeII]_{12,8\mu m}$ e $[ArIII]_{8,9\mu m}/[ArII]_{6,9\mu m}$. As faixas de temperatura da estrela central de cada nanopartícula também foram obtidas. Finalmente, concluiu-se que existe uma certa proporcionalidade entre as razões iônicas e a temperatura das estrelas, mas essa previsão pode ser imprecisa para algumas faixas de temperatura devido ao comportamento da curva formada pela relação entre a temperatura e as razões.

Keywords. (ISM:) planetary nebulae: general – Infrared: stars – Stars: AGB and post-AGB

1. Introduction

Planetary Nebulae (PNe) represent the final stage in the evolution of low- and medium-mass stars (1–8 solar masses), when mass loss during AGB phase forms envelopes of gas and dust that become ionized by the ultraviolet radiation of the central heating star. These objects are fundamental to the chemical enrichment of the interstellar medium, releasing elements such as C, O, and N, and also act as laboratories for the study of the interaction between stellar winds, gas dynamics, and dust properties. Emission lines allows for the investigation of both ionization and the role of dust in energy balance and the formation of complex structures. The infrared spectroscopy of PNe is particularly important, as it gives us important information to analyze the chemical composition, characterize cosmic dust and reveal internal structures that are obscured in visible light.

In this work we analyze the infrared spectra from 6 compact (apparent diameter < 4") PNe, PN M 1-37, PN M 1-12, PN H 1-19, PN H 1-23, Hen 2-406 and NGC 6833, observed with the Spitzer Space telescope, selected from a sample of 157 Galactic PNe described by Stanghellini et al., 2012.

2. Methodology

Low-resolution spectra (5-14 μm) were obtained for each PNe, available at CASSIS [1] (Lebouteiller et al., 2011), a database of Spitzer Spectra already reduced for science. An infrared spectra analysis were conducted, identifying the emissions contained in each spectra that were previously observed by others in the literature. Once a first inspection were carried, we decomposed each spectra using the PAHFIT Spitzer spectra decomposition tool (Smith et al., 2007), designed to decompose the low-resolution mid infrared (MIR) Spitzer IRS (Infrared Spectrograph) spectra into emission lines, molecular and dust components.

The Cloudy photoionization code version 17.02 (Ferland et al., 2017) was used to simulate a set of fictional PNe by varying the H density, luminosity, dust mass and effective temperature parameters. The simulation produces a spectra for each fictional PNe, allowing the retrieval of information like the emission line fluxes. Here we opted to choose a default solar-like abundance for the modeled PNe and varied the luminosity in different colors, as shown in Figure 1 and Figure 2.

One important characteristic can be retrieved from ionic line ratios: the ionization potential of the radiation emitted by the central star of the PN (CSPN) and also the effective temperature of the CSPN. The ionic ratio from MIR lines $[NeIII]_{15.5\mu m}/[NeII]_{12.8\mu m}$

[1] https://cassis.sirtf.com/

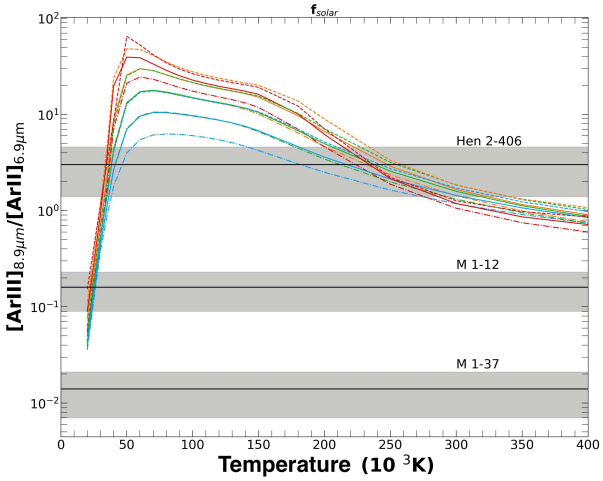

Figure 1. $[ArIII]_{8.9\mu m}/[ArII]_{6.9\mu m}$ as a function of T_{eff}. Black horizontal line represents M 1-37, M 1-12 and Hen 2-406 ratio values, gray band indicates the uncertainty. Colored curves represent values of log n_H (cm) = 2, 3, 4 and 5 for blue, green, orange and red, respectively. The solid and dashed dot-dashed curves indicate log $(L_\star/L_\odot)$ = 2, 3 and 4. Source: Author

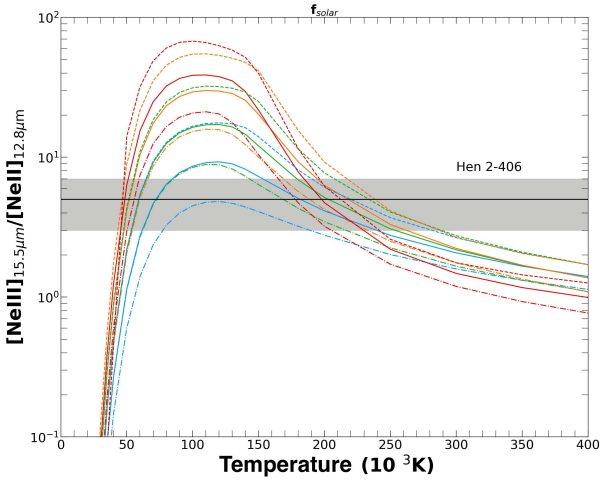

Figure 2. $[NeIII]_{15.5\mu m}/[NeII]_{12.8\mu m}$ as a function of T_{eff}. The colors and line designations are the same as in Figure 1 Source: Author

is a strong diagnosis of the ionization state, as these lines are not greatly affected by extinction (Groves et al., 2008). The ratio $[ArIII]_{8.9\mu m}/[ArII]_{6.9\mu m}$ is used in determining the temperature because of the similar ionization potential of both lines. Ionic ratios from both Ne and Ar were retrieved from the spectra of the 6 PNe selected and compared to the values from the fictional PNe to verify if they are indeed good for determining physical parameters.

3. Results

We estimated the possible T_{eff} range for each one considering that the PN has the required line intensities for both ionic lines. Only Hen 2-406 and NGC 6833 had both $[NeIII]_{15.5\mu m}$ and $[NeII]_{12.8\mu m}$ lines present in their spectra. The rest of the sample had only the Ar lines.

$[NeIII]_{15.5\mu m}/[NeII]_{12.8\mu m}$ by T_{eff} plot is shown in Figure 2, exhibiting a maximum ratio peak around ~100 kK, with a value of 80. As expected, the ratio grows with temperature until this point, as the high energy photons produce a more abundant fraction of Ne^{++}. The decreasing in the ratio for values beyond the peak is due to the promotion of these ions to higher ionization states, reducing the quantity of both Ne^{++} and Ne^{+}. The ratios from modeled PNe shows the behavior for different values of luminosity and using a solar abundance.

A similar behavior happens between $[ArIII]_{8.9\mu m}/[ArII]_{6.9\mu m}$ and T_{eff}. The ionic ratio, after reaching it's maximum value around ~50 kK, decreases in a slow pace forming a plateau, and after that decreasing again to values getting closer to zero. The plateau makes it difficult to estimate temperature using the ionic ratio because it creates a region where similar ratio values represents a wide temperature range, as can be seen in Ar ratio values between 6 and 12. There was one for PN M 1-37, the $[ArIII]_{8.9\mu m}/[ArII]_{6.9\mu m}$ ratio was below the available curves range from the modeled PNe and was not possible to estimate it's T.

Because of the maximum value in both ionic ratios, the same ion ratio value repeats for two T_{eff} value, making the relation between these two physical parameters not very reliable. The correct T_{eff} value can only be estimated by considering other characteristics of the nebula that support whether its star is very hot (>150kK) or not.

Table 1. Table of literature temperatures with temperatures estimated by ratios. Temperatures are T_Z (Zanstra Temperature), T_{eff} (Effective Temperature) and T_{EB} (Energy Balance Temperature). *Inference was not possible. (a) (Preite-Martinez et al., 1989)), (b)(Ratag et al., 1997b), (c) (Weidmann et al., 2020), (d) (Lykou et al., 2020).

PN	T_Z $(10^3 K)^{(c)}$	T_{eff} $(10^3 K)$	T_{EB} $(10^3 K)^{(a)}$
M 1-37	31.5	$29^{(b)}$	51.8
M 1-12	32	–	–
Hen 2-406	–	$102.5^{(b)}$	95.2
H 1-19	–	$52^{(d)}$	51.9
H 1-23	–	$52^{(c)}$	–
NGC 6833	–	$38^{(c)}$	–

PN	T_{Ne} $(10^3 K)$	T_{Ar} $(10^3 K)$
M 1-37	–	*
M 1-12	–	20-30
Hen 2-406	40-70 ou 170-300	30-45 or 200-300
H 1-19	–	30-45 or 180-280
H 1-23	–	35-50 or 180-280
NGC 6833	35-60 ou 250-350	30-45 or 180-280

References

Ferland, G. J. et al. 2017, Rev. Mexicana Astron. Astrofis., 53, 385
Groves, B., Nefs, B., Brandl, B. 2008, MNRAS, 391, L113
Lebouteiller, V., Barry, D. J., Spoon, H. W. W., Bernard-Salas, J., Sloan, G. C., Houck, J. R., Weedman, D. W. 2011, ApJS, 196, 8
Lykou, F., Zijlstra, A., Parker, Q. A. 2020, Galaxies, 8, 51
Preite-Martinez, A., Acker, A., Koeppen, J., Stenholm, B. 1989, A&AS, 81, 309
Ratag, M. A., Pottasch, S. R., Dennefeld, M., Menzies, J. 1997b, A&AS, 126, 297
Smith, J. D. T. et al. 2007, ApJ, 656, 770
Stanghellini, L., García-Hernández, D. A., García-Lario, P., Davies, J. E., Shaw, R. A., Villaver, E., Manchado, A., Perea-Calderón, J. V. 2012, ApJ, 753, 172
Weidmann, W. A., Mari, M. B., Schmidt, E. O., Gaspar, G., Miller Bertolami, M. M., Oio, G. A., Gutiérrez-Soto, L. A., Volpe, M. G., Gamen, R., Mast, D. 2020, A&A, 640, A10